High Modulus and High T_g Thermally Stable Polymers from Di-*p*-ethynylbenzoyl Ester Monomers: Synthesis, Solid State Polymerization, Processing, and Thermal Properties

Anastasios P. Melissaris and Morton H. Litt*

Department of Macromolecular Science, Case Western Reserve University, Cleveland, Ohio 44106

Received July 21, 1993; Revised Manuscript Received January 19, 1994®

ABSTRACT: Seven novel *p*-ethynylbenzoyl ester momoners (EBEs) have been synthesized in high yield and purity and characterized by GPC and X-ray, FTIR, Raman, and ^{1}H NMR spectroscopy. The monomers are crystalline. Five of the monomers polymerized without melting. Thermal polymerization in N_2 produced highly cross-linked resins with polymerization exotherms centered between 204 and 250 °C. The monomers are liquid crystalline or crystalline during polymerization and yield polymers retaining some order. They polymerize to high conversion in spite of their rigid matrix, which was attributed to the fact that their ethynyl groups interdigitate to a certain degree. Methylhydroquinone- and chlorohydroquinone–bis(4-ethynylbenzoate) melt to a nematic mesophase just before they polymerize. The monomers polymerized in the solid state (crystalline) exhibited little or no polymerization shrinkage (0–2.3%). 4,4′-Dihydroxybiphenyl–bis-(4-ethynylbenzoate) showed zero polymerization shrinkage. A new processing technique was used to polymerize the monomers which neither melt or have a softening point. EBEs were thermally polymerized under moderate pressure to yield high modulus, cohesive polymer plates. Polymer plates could be made from 2,6-dihydroxynaphthalene–, 1,5-dihydroxynaphthalene–, and 4,4′-dihydroxybiphenyl–bis(*p*-ethynylbenzoate) that were void free and had storage moduli, E', from 4.5 to 4.8 GPa at room temperature. Using DMA and TMA it was found that all polymers except the 2,6-dihydroxynaphthalene–ester had T_g's from 345 to 440 °C, 50 to 140 deg higher than their polymerization (processing) temperatures! EBE polymers have very high E's and T_g's, much higher than those of normal amorphous cross-linked polymers, because they are highly cross-linked rodlike materials. Using TGA under N_2, the polymers showed a 5% weight loss between 446 and 485 °C, a maximum decomposition temperature from 554 to 598 °C, and anaerobic char yield of 60 to 66% at 800 °C. Isothermal aging for poly(hydroquinone–bis(*p*-ethynylbenozate)) showed that the polymer retained more than 70% of its initial weight after 100 h at 320 °C in air. Of all the polymers, poly(4,4′-dihydroxybiphenyl–bis(*p*-ethynylbenzoate)) showed the best combination of thermomechanical and thermal properties (4.5-GPa storage modulus at room temperature, T_g over 415 °C, and initial decomposition temperature over 470 °C).

Introduction

One of the conventional approaches to the design of improved structural materials is reinforced polymer composite technology. The transfer of stresses from a matrix polymer to reinforcing entities such as rigid particles, chopped fibers, or continuous filament has been a very effective technique for improving mechanical properties of polymeric materials. The problem in using high T_g polymers in composites is that the usual monomers are amorphous and must be polymerized at temperatures above the final T_g in order to get high conversion and good mechanical properties in the matrix. If the polymer is cross-linked, two further problems arise. First, as the polymerization continues the matrix shrinks, stressing the matrix/fiber interfacial bond. Second, as the composite cools from the high curing temperature, the matrix shrinks further. Since its coefficient of expansion is higher than that of the fiber, the shrinkage puts further stress on the interfacial bond. The stress can sometimes become so great that the composite loses its integrity. These problems can be minimized or avoided by polymerizing self-organizing systems. Monomers with terminal functional groups which form smectic liquid crystal layers are needed. Because all the terminal functional groups are packed into a very small fraction of the total volume, they can polymerize well to high conversion without needing to diffuse to find other reactive ends. Thus a high T_g does not prevent high conversion at low temperatures. Similarly, polymerization in an ordered phase means that the molecules are well packed even before polymerization, so there should be little or no shrinkage.

A series of liquid crystal monomers bis(ω-(acryloyloxy)-polymethylene) ethers of 4,4′-biphenol, were synthesized and studied by Litt et al.[1] The monomer with a trimethylene spacer polymerized between 60 and 80 °C and gave a crystalline polymer with a T_g at 1 Hz of 185 °C with a volume shrinkage of about 3%; with an undecamethylene spacer the monomer and the polymer had the same density! However, to obtain high T_g polymers, monomers should contain the moieties which are used to generate rigid rod nematic liquid crystal polymers. These include aromatic polyesters,[2] polyimides,[3,4] poly(bis(benzoxazoles)),[5] thiazoles,[6] quinolines,[7] biphenyls,[8] and naphthalenes.[9] The most important restriction is in the nature of the polymerizable functionality.

Acetylene terminated resins have generated much interest as candidates for high performance matrix resins for aircraft and aerospace applications. This interest has hinged upon several attractive features of the material including (1) a chain addition cure mechanism, which promises void-free laminates,[10] (2) a thermally initiated cure without added catalyst or hardener, which implies long shelf life, (3) batch to batch homogeneity approaching that of the thermoplastics,[11] and (4) high glass transition temperatures[12] and thermal stabilities made possible by the incorporation of wholly aromatic precursors into a heavily cross-linked polyene network. The ethynyl group has been widely used as a reactive agent for a variety of monomers and oligomers such as ether–ketone–sulfones,[13,14] phenylquinoxalines, with pendant ethynyl

® Abstract published in *Advance ACS Abstracts*, April 1, 1994.

0024-9297/94/2227-2675$04.50/0

Scheme 1. Interdigitation of the Ethynyl Groups and Their Polymerization

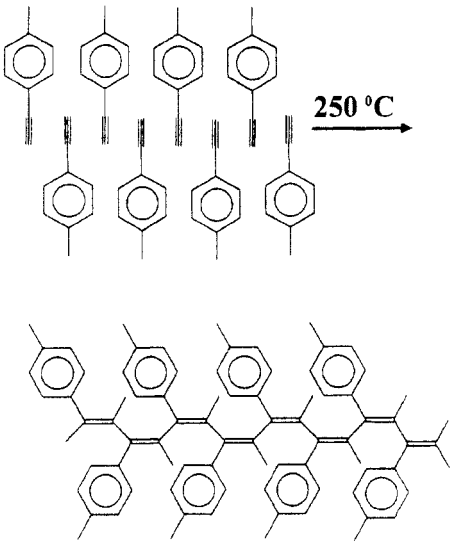

groups,[15] phenyl-as-triazines,[16] and Schiff bases[17] for obtaining improved high-temperature structural resins.

We believe that the acetylene terminal group as para substituent in aromatic rigid rod monomers is a good candidate as a polymerizable functionality for the following reasons. An acetylene terminal group has a van der Waals cross-section that is half or less than half that of the aromatic groups that will make up the bulk of the molecule and it is aligned along the monomer long axis. Thus, rigid linear aromatic structures with terminal *p*-ethynyl groups could pack smectically with the acetylene groups interdigitated. This is shown in Scheme 1. The separation between the molecules oriented as in Scheme 1 is about 6.5–7 Å. The van der Waals diameter of the acetylene group is about 3.3–3.5 Å, so it could interdigitate easily. The interdigitated acetylenes probably lie between two rows of acetylenes rather than within one row as shown. Interdigitation implies that the head of one acetylene group is next to the tail of the neighboring one. Thus normal head-to-tail polymerization should proceed readily. Polymerization should occur perpendicular to the direction shown in the above illustration. The intermolecular distance perpendicular to the aromatic ring is usually about 4–4.5 Å, which is just about the repeat length for two acetylene units joined in cisoid conformation. What is most intriguing is that this polymerization pathway should stitch the lamellae together, since each neighboring acetylene residue is from a different lamella. There should be very little volume contraction since the material is already liquid crystalline. The final polymers should have high moduli and be very thermally stable.

The objective of this research was to develop new monomers which could polymerize in the solid or liquid crystalline state at moderately elevated temperatures (130–250 °C) and yield highly cross-linked thermally stable resins suitable as matrices for high temperature composites. *p*-Ethynyl substituted rodlike monomers have not been studied in the past because of problems arising from the para substitution. Such monomers do not melt and have very low solubility in common organic solvents, which makes their processing very difficult. Despite the reported difficulties we decided to develop processing conditions for the monomers and study the polymer thermomechanical properties. These polymers should have excellent thermomechanical properties for the reasons discussed in the last paragraph.

Chart 1. Chemical Structures of Di-*p*-ethynylbenzoyl Esters, EBEs

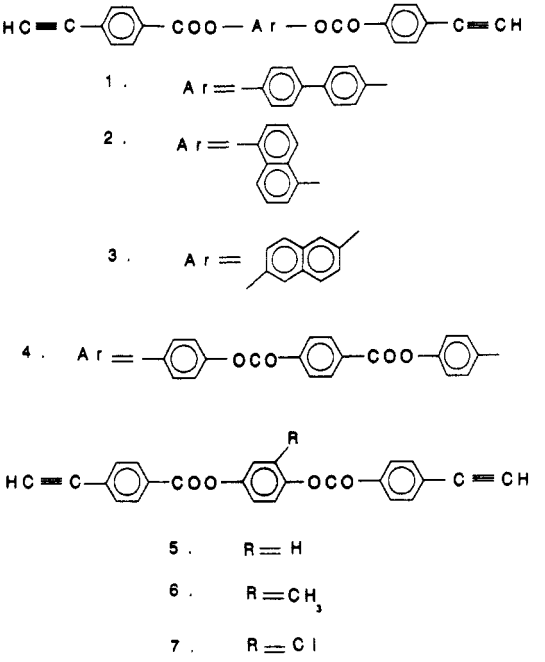

Table 1. Yield, Purity, and Densities of 1–7 and 1p–7p

			density (g/cm³)		
sample	yield (%)	purity (%)	monomer	polymer	Δ(*d*) (%)
1	93	98	1.28	1.28	0
2	95	99	1.25	1.26	0.8
3	98	98.5	1.22	1.25	2.4
4	97	98.5	1.28	1.30	1.5
5	99	99	1.25	1.27	1.6
6	99	99	1.24	1.28	3.1[a]
7	97	98.5	1.27	1.30	2.3[a]

[a] Monomers became nematic and flowed before polymerizing.

Results and Discussion

Monomer Preparation and Characterization. The chemical structures of the di-*p*-ethynylbenzoyl esters synthesized, 1–7, are shown in Chart 1. 1–7 were prepared in high yield and high purity (Table 1) by reacting *p*-ethynylbenzoyl chloride (EBC) (2 mol) with the appropriate biphenol (1 mol), using 4-(*N*,*N*-dimethylamino)-pyridine as the hypernucleophilic agent and triethylamine as the acid acceptor. 4 was synthesized by the reaction of hydroquinone–mono(*p*-ethynylbenzoate) (2 mol) (MEBH) with terephthaloyl chloride (1 mol). For the synthesis of MEBH, EBC (1 mol) was reacted with an excess of hydroquinone (HQ) (3 mol) in the presence of pyridine. MEBH was prepared in high purity and yield because we took advantage of two facts; MEBH is much less nucleophilic toward EBC than toward HQ and the excess of HQ could be selectively removed by washing the residue several times with warm water. *p*-Ethynylbenzoyl chloride (EBC) was quantitatively synthesized by an economical and simple synthetic route developed in our laboratory;[18] it was stored at −20 °C after its preparation because it self-polymerizes at room temperature.

2,6, and 7 dissolved in chloroform, dichloromethane, acetone, and tetrahydrofuran. 3–5 were soluble in warm DMAc, DMF, DMSO, and *sym*-tetrachloroethane (caution: toxic). 1 was found to be soluble only in warm *sym*-tetrachloroethane. 1–7 had a light tan or light yellow color. However, upon standing at room temperature in the presence of light over a long period of time they darkened, probably due to slow photopolymerization of the acetylene group in the solid state (generation of conjugated bonds).

Table 2. ^{1}H NMR Data for EBEs

monomer	chemical shifts (δ, ppm) and assignments
1	insoluble even in warm DMSO
2	4.40[a] (s, 2H, acetylene), 7.40–7.60 (m, 4H, aromatic of naphthalene ring), 7.65–7.80 (d, 4H, aromatic ortho to ethynyl), 7.85–7.90 (d, 2H, aromatic of naphthalene ring of C_4), 8.10–8.20 (d, 4H, aromatic ortho to carbonyl)
3	4.30[a] (s, 2H, acetylene), 7.25–7.35 (d, 2H, aromatic of naphthalene ring of C_3), 7.70–7.80 (d, 4H, aromatic ortho to ethynyl), 7.95 (s, 2H, aromatic of naphthalene ring of C_1), 8.00–8.15 (d, 2H, aromatic of the naphthalene ring of C_4), 8.20–8.30 (d, 4H, aromatic ortho to carbonyl)
4	4.20[a] (s, 2H, acetylene), 7.30 (s, 8H, aromatic ortho to oxygen), 7.50–7.60 (d, 4H, aromatic ortho to ethynyl), 8.15–8.25 (m, 8H, aromatic ortho to carbonyl)
5	4.30[a] (s, 2H, acetylene), 7.30–7.40 (s, 4H, aromatic ortho to oxygen), 7.55–7.65 (d, 4H, aromatic ortho to ethynyl), 8.00–8.10 (d, 4H, aromatic ortho to carbonyl)
6	2.26[b] (s, 3H, methyl of MeHQ), 4.18 (s, 2H, acetylene), 7.25–7.40 (m, 3H, aromatic of MeHQ ring), 7.65–7.85 (m, 4H, aromatic ortho to ethynyl group),8.15–8.25 (d, 4H, aromatic ortho to carbonyl)
7	3.95[c] (s, 2H, acetylene), 7.25–7.45 (m, 3H, aromatic of ClHQ ring), 7.60–7.75 (m, 4H, aromatic ortho to ethynyl), 8.10–8.30 (d, 4H, aromatic ortho to carbonyl)

[a] In DMSO-d_6 at 60 °C. [b] In acetone-d_6 at room temperature. [c] In chloroform-d at room temperature.

The purity of all monomers was checked by GPC and ranged between 98 and 99.5% (Table 1). Their chemical structures were confirmed by IR, Raman, and ^{1}H NMR spectroscopy. The IR spectra of **1–7** exhibited intense absorption bands in the region of 1750 and 1250 cm^{-1}, which were associated with the ester structure (C=O and C—O stretching, respectively). The acetylene group showed characteristic IR absorption bands at 3298 and 627 cm^{-1} correlated with the carbon(sp)–hydrogen stretching and bending vibrations. The Raman spectra of all the monomers showed a sharp absorption band at 2108 cm^{-1} due to the carbon–carbon triple bond stretching mode. The ^{1}H NMR spectra of the monomers (Table 2) showed a singlet at 3.95 ppm in $CDCl_3$, 4.18 ppm in acetone-d_6, and 4.20–4.40 ppm in DMSO-d_6 at 60 °C, which was attributed to the acetylene protons. The ^{1}H NMR spectrum of **1** could not be obtained because of its very low solubility in DMSO. The densities of the monomers ranged from 1.22 to 1.28 g/cm^{-3} (Table 1). The monomers were examined by X-ray and hot stage cross-polarized microscopes and were found to be crystalline. Only **6** and **7** exhibited "melting" points. They polymerized immediately after transition to a nematic mesophase. The others polymerized in the solid state.

Monomer Polymerization and Curing. The thermal polymerization of arylacetylene monomers is considered to be chain polymerization by the conventional radical mechanism.[19] The rate of polymerization was found to increase with the addition of radical initiators such as benzoyl peroxide.[19] ESR signals are intense during the polymerization; their intensity increases with conversion, attains a maximum, and then decreases.[20]

Table 3. DSC Data for EBEs

monomer	melting point[a] (°C)	T_i[b] (°C)	T_{max}[c] (°C)	T_f[d] (°C)	ΔH_{polym} (kJ/mol)	ΔH_{polym} (J/g)
1		143	220	302	153	347
2		136	258	298	187	450
3		142	211	300	169	407
4		171	249	319	154	254
5		158	227	309	177	483
6	167	174	204	313	164	431
7	173	181	218	319	196	490

[a] Transition to nematic structure. [b] Initiation temperature for polymerization. [c] Temperature of maximum polymerization rate. [d] Completion temperature for polymerization.

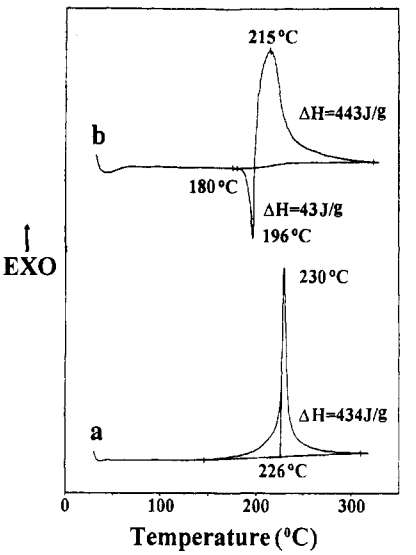

Figure 1. DSC thermograms of **5** (a) and **7** (b) at 15 °C/min under N_2.

The polymers are denoted by appending **p** to monomer number, **1p–7p**. Highly cross-linked resins, **1p–7p**, were obtained by heating the corresponding monomers **1–7** at 220 °C for 30 min and subsequently at 250 °C for 1.5 h (postcuring) in N_2. It is noteworthy that the polymerization went to completion (loss of all characteristic ethynyl bands in the IR spectra; see below) when the monomers were heated in N_2 for 1.5 h at temperatures between 200 and 220 °C. However, postcuring is necessary in order to get highly cross-linked resins with improved thermal and mechanical properties.

The curing behavior of **1–7** was examined by DSC (15 °C/min in N_2). The DSC data for all monomers are listed in Table 3. From this table it can be seen that **1–5** polymerized in the crystalline (solid) state (Figure 1a) while **6** and **7** polymerized in a lower ordered state immediately after the k–n (or s–n) transition (Figure 2). The DSC thermograms of **6** and **7** exhibited an endotherm just before the polymerization exotherm (Figure 1b). The polymerization exotherms peaked between 204 and 258 °C. **2** had the lowest initial polymerization temperature T_i = 136 °C, while **4** and **7** had the highest completion temperature of polymerization: T_f = 319 °C. For **4** this is attributed to the lower concentration of ethynyl groups compared to the other monomers. It was found that all monomers except **2** and **4** exhibited a T_{max} between 204 and 228 °C, which indicates that the chemical structure of the aromatic diols did not significantly influence the curing behavior. The T_g's of the cross-linked polymers **1p–7p** could not be detected by DSC because they were highly cross-linked and the change in C_p was very small.

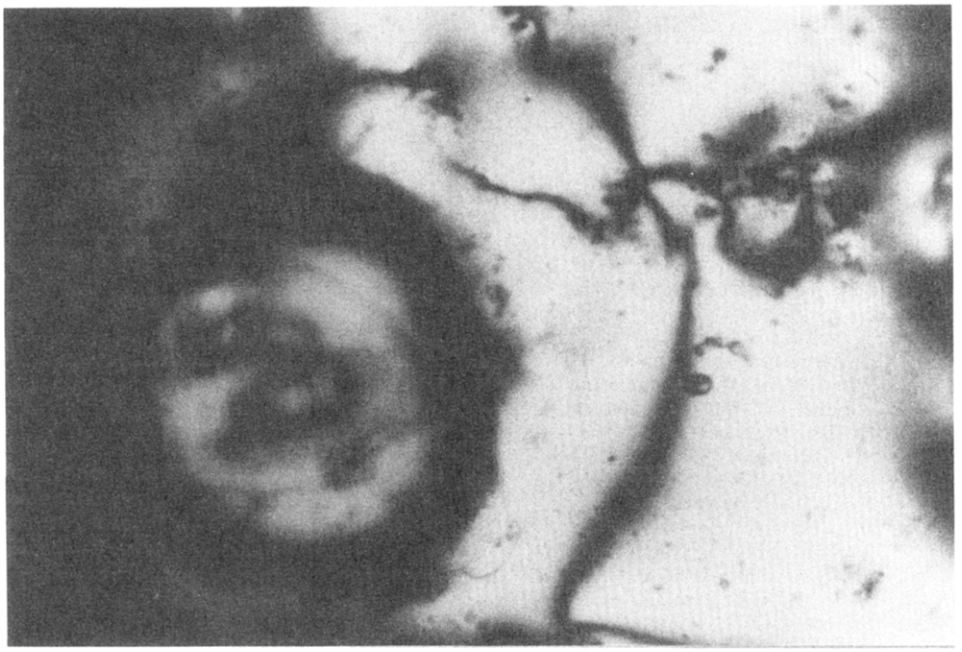

Figure 2. Optical microphotograph of **6** after heating for 2 h at 190 °C.

Table 4. Lamellar Spacing, Interdigitated Spacing, and Calculated Length from H_α to H_ω for 1–5

monomer	lamellar spacing (Å)[a]	calcd length (H_α–H_ω, Å)[a]	calcd intedigitated spac (Å)[a]
1	25.7	27.3	24.0
2	17.5	23.2	19.9
3	21.6	25.1	21.8
4	22.6[b]	35.9	32.6
5	22.1	23.1	19.8

[a] Spacing corresponds to the molecular length if molecules are perpendicular to the lamellar plane. [b] Molecules probably are tilted.

Combining the WAXD data for **1–5** with the data obtained from computer modeling ("Alchemy" software) revealed that **1–3** and **5** interdigitate to a certain degree at room temperature. **1–3** possibly have a high degree of interdigitation. The calculated interplanar distances for **1–5** from WAXD spectra and the monomer end-to-end distances from "Alchemy" are listed in Table 4. The calculated end-to-end distances of **1–5** except **4** are larger than their measured lamellar spacings. (**2** can be indexed in an orthorhombic unit cell, which usually means that the monomer axis is vertical.) **1** and **3**, which have the closest match between calculated and measured spacings, have the lowest T_{max} of the five monomers which polymerized without melting. While it is possible that the monomers are tilted with respect to the lamellar plane, the minimum tilt to get a fit without interdigitation is 30° from the vertical. It is more reasonable to postulate 2–5-Å interdigitation at room temperature. We hope to address this question more deeply in the future.

Of the monomers that polymerized in the solid state, **3** exhibited the most attractive polymerization features. It started curing at 142 °C with a T_{max} of only 211 °C! This behavior could be rationalized if the molecules of 2,6-bis(4-ethynylbenzoyloxy)naphthalene in the solid state are packed in a way which facilitates the polymerization. The *d* spacing for **3**, Table 4, of 21.6 Å is almost perfect for full interdigitation of the ethynyl groups. That is calculated to be 21.8 Å for this monomer.

Optical Microscopy. Optical microscopy was very useful in elucidating the thermal transitions and polymerization behavior of **6** and **7**. Heating and cooling rates between 5 and 10 °C/min were used during the microscope observations. Sometimes fast heating rates were needed to define the general behavior of the monomers. These monomers are highly reactive systems and substantial reaction occurred at the lower heating rates. **6** and **7** showed a thermotropic nematic liquid crystalline mesophase and thermally polymerized in the nematic phase. The nematic texture was maintained to a degree in the cross-linked solid state. The cross-linking and solidification of **6** and **7** were both time and temperature dependent; slower heating rates resulted in a lower solidification temperature. The DSC curves of **6** and **7** were characterized by a sharp endotherm followed by a polymerization exotherm. When **6** was heated isothermally at 180–190 °C, the schlieren nematic texture was retained. After 2 h of heating at 190 °C (complete polymerization), the sample retained a lower degree of the schlieren nematic structure (Figure 2). The transitions of **7** were not as clear as those of **6**. This could possibly be because the recrystallized chlorohydroquinone (technical grade) was not of as high purity as the methyl hydroquinone.

1–5 did not melt. They polymerized in the crystalline phase. Polymers of **1** and **2** showed poorly organized crystallinity. When **1** was heated between two glass plates (absence of air) on the hot stage, the cross-linked polymer, **1p**, had the same birefringence as the monomer (Figure 3). That indicates that **1p** retains orientational order.

FTIR, Raman, and DSC Study. Three techniques, DSC, IR, and Raman were used in order to find out whether **1–7** polymerized to high conversion. Using DSC it was found that **1–7** are polymerized completely after 2 h at 220 °C. **1** and **6** were completely polymerized after 2 h at 190 °C. The IR spectra of **1p–7p** lost the characteristic absorption bands of the monomers at 3298–3300 and 627 cm^{-1} due to carbon(sp)–hydrogen stretching and bending (acetylene group). This is shown for **1** and **1p** in Figure 4.

The sharp absorption band in the Raman spectra of **1–7** at 2106–2108 cm^{-1} due to carbon(sp)–carbon(sp) stretching completely disappeared from the spectra of the polymerized resins, showing 100% reaction of the ethynyl groups. Figure 5 shows the Raman spectra of **1** and **1p** as representative of this series of monomers and polymers.

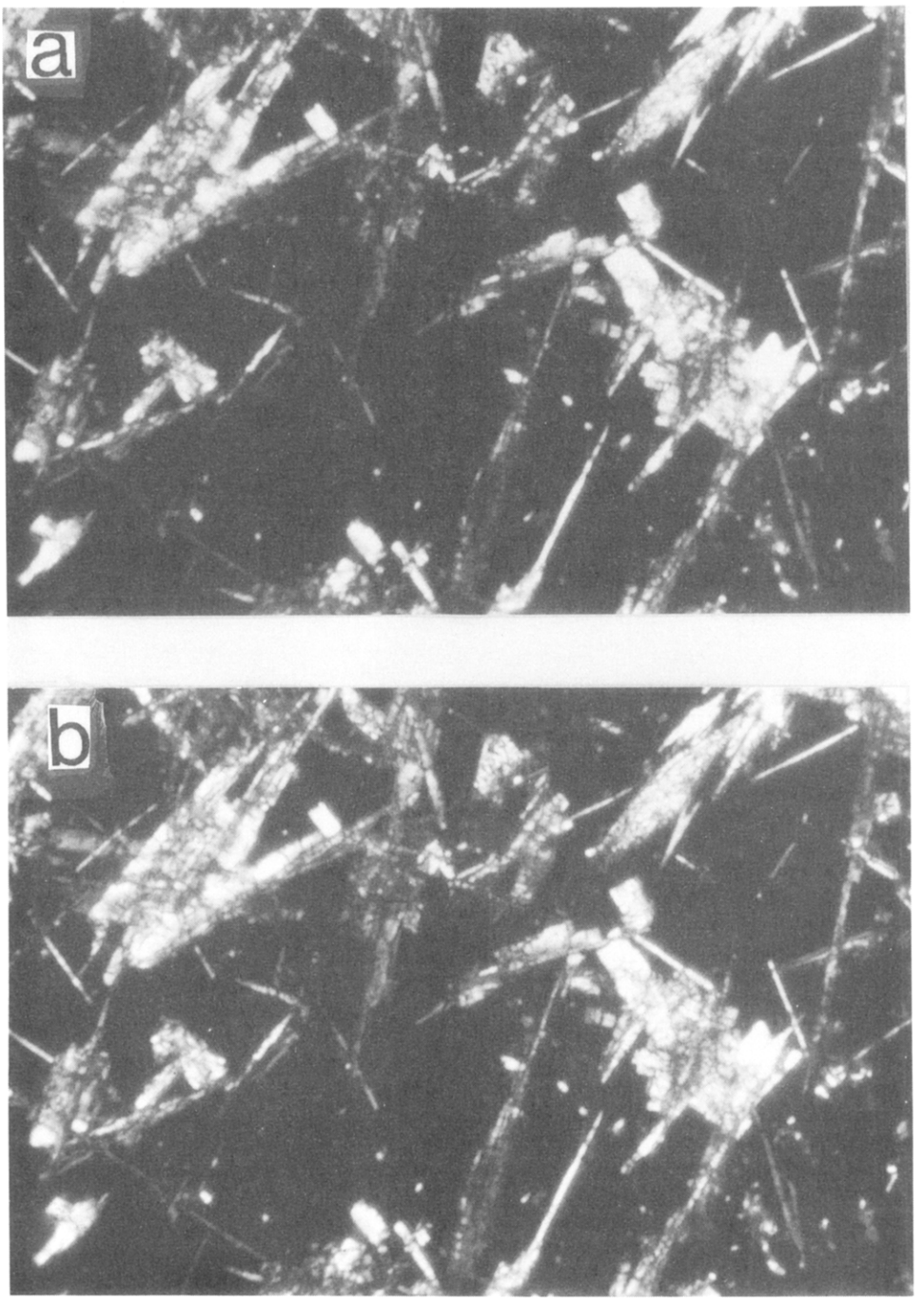

Figure 3. Optical microphotographs of **1** (a) and of **1** after heating to 310 °C at 10 °C/min in the absence of air (b).

Different samples of **1**, as powders or pressed pellets, were heated under N_2 at different temperatures and periods of time to get samples with different degrees of polymerization. Figure 4 shows the IR spectra of **1** (a) and of **1** after heating as a powder under N_2 for 1 h at 210 °C (b) and for 30 min at 200 °C and 2 h at 250 °C (c). The DSC thermograms and WAXD spectra of the same samples are shown in Figures 6 and 7. Figure 4a shows medium absorption bands at 3298 and 627 cm^{-1} due to the C(sp)–H stretching and bending vibrations of the acetylene groups. The same bands with lower intensity appear in Figure 4b but completely disappear from Figure 4c. The very weak band at 3051 cm^{-1} in Figure 4a becomes more intense in Figure 4b. It was attributed to the generation of a polyene structure ($C(sp^2)$–H stretching).

Combining IR and DSC data from Figures 4 and 6, it can be seen that the characteristic bands of the ethynyl group at 3298 and 627 cm^{-1} in the IR spectra (Figure 4a,b) are inversely correlated with the extent of reaction at 150–260 °C (Figure 6a,b). After polymerization, **1** showed no acetylene absorption bands (Figure 4c), and its DSC (Figure 6c) had no polymerization exotherm at 150–260 °C. **1** postcured at 250 °C shows a very weak exotherm at 300–400 °C (Figure 6c). This was attributed to further reactions of a rearranged polyene structure. The rearrangements probably happened during the extended heating at 250 °C since the DSC thermograms (Figure 6a,b) do not show the weak exotherm between 300 and 400 °C.

1 is a crystalline material which can be polymerized in the solid state. When **1** is polymerized as a powder to 95% conversion (based on ΔH of polymerization of Figure 6b), some monomer crystallinity remains (Figure 7b). Additional curing or postcuring destroys the crystallinity. The fact that **1p** retains the same birefringence as **1** (Figure 3) implies that this polymer retains a certain amount of

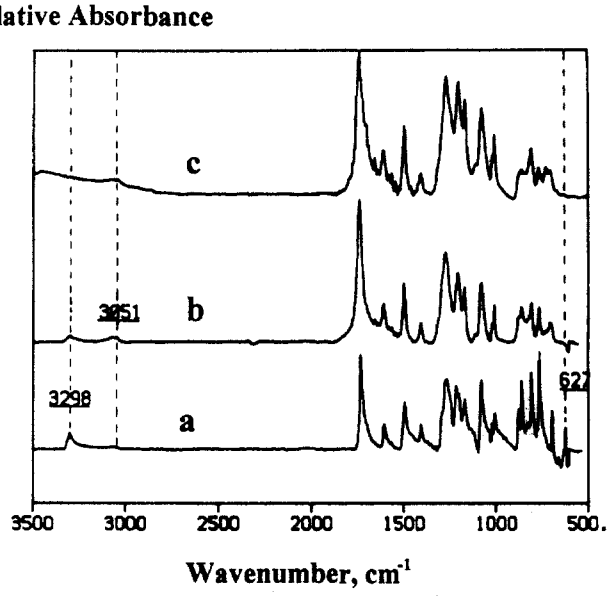

Figure 4. IR spectra of 1: monomer (a); 1 after heating for 1 h at 210 °C in N_2 (b); 1 after heating for 30 min at 200 °C and for 2 h at 250 °C in N_2 (c).

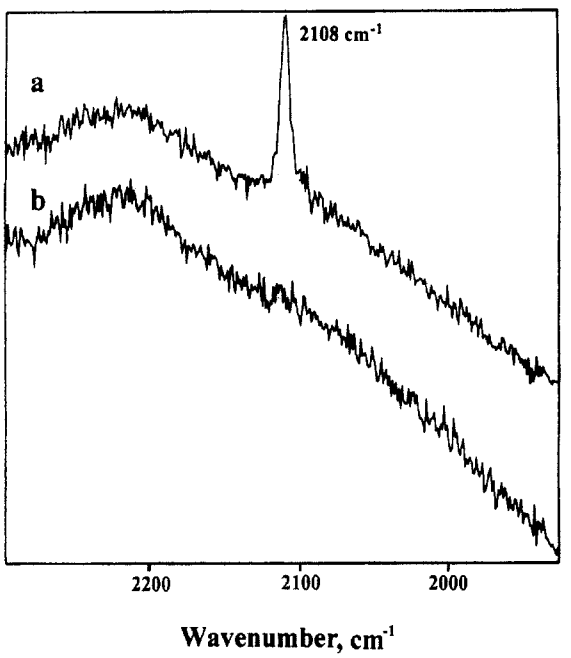

Figure 5. Raman spectra of 1 (a) and of 1 after heating at 200 °C for 30 min and for 2 h at 250 °C in N_2 (b).

local order. When 1 was polymerized in a pressed plate form under 1 kpsi at 300 °C for 1 h, a semicrystalline polymer was obtained (Figure 8).

Density and Polymerization Shrinkage. The densities of **1**–**7** and **1p**–**7p** were measured and are listed in Table 1. For **1**–**7** they ranged between 1.22 and 1.28 and for **1p**–**7p** between 1.25 and 1.30 g/cm.[3] Table 1 shows that **1p** had the same density as **1**; there was zero polymerization shrinkage. **2p** shrank only 0.8%. **3**–**5** polymerized in the solid state shrank between 1.5 and 2.3%. **6** and **7** had higher shrinkages of 3.1 and 2.3%. Note that the shrinkages observed for **1**–**7** are much lower than those observed for epoxy–aromatic amine systems (8–9%)[21] or for acrylate networks (11–15%).[22] Due to low polymerization shrinkage **1**–**7** are expected to be good candidates for the fabrication of high temperature composites with improved mechanical properties because

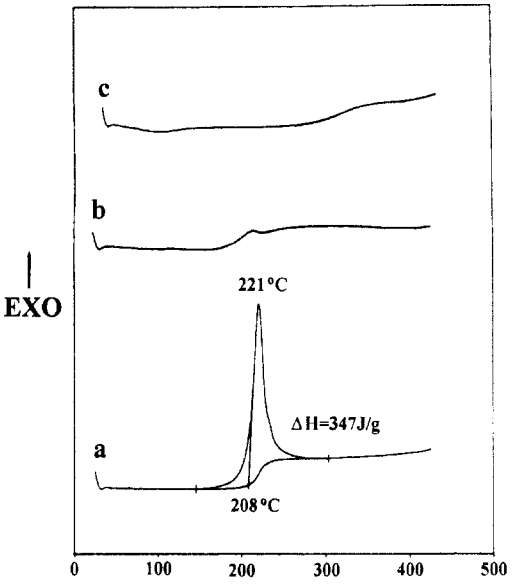

Figure 6. DSC thermograms of 1: monomer (a); monomer after heating for 1 h at 210 °C in N_2 (b); monomer after heating for 30 min at 200 °C and for 2 h at 250 °C in N_2 (c). (The DSCs were recorded in N_2.)

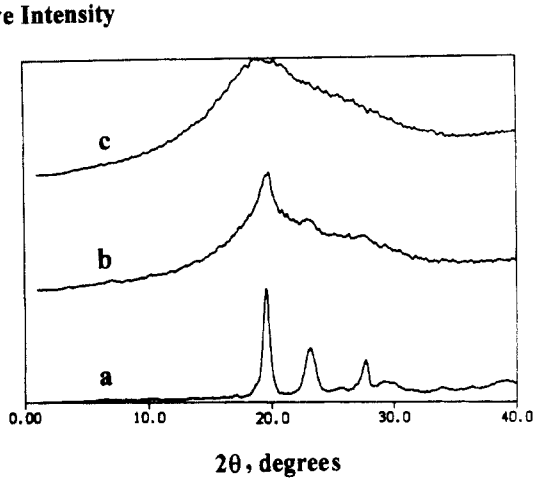

Figure 7. WAXD spectra of 1: monomer (a); monomer after heating for 1 h at 210 °C in N_2 (b); monomer after heating for 30 min at 200 °C and for 2 h at 250 °C in N_2 (c).

interfacial bond stresses between the matrix and fiber will be minimized.

Processing. We were interested in developing a processing technique for **1**–**5** because they should have high moduli, little or no polymerization shrinkage, and very low thermal expansion. Films could not be made by casting a monomer solution and evaporating the solvent, because the monomers are highly crystalline. Normal melt processing techniques could not be used because **1**–**5** do not have melting or softening temperatures. A new processing technique for the fabrication of polymeric plates was developed that involves solid state polymerization under moderate pressure. Because of manpower limitations we did not optimize the processing conditions for all monomers. **1**–**3** were processed under well-defined conditions; see Table 5. **4** and **5** were processed on the basis of the conditions listed in Table 5; these conditions were not optimal, as **4p** and **5p** were neither very cohesive nor void free. No attempt was made to optimize the processing conditions for **6** and **7**. These monomers melted to a nematic mesophase before they polymerized. Their processing conditions will be studied in the near future.

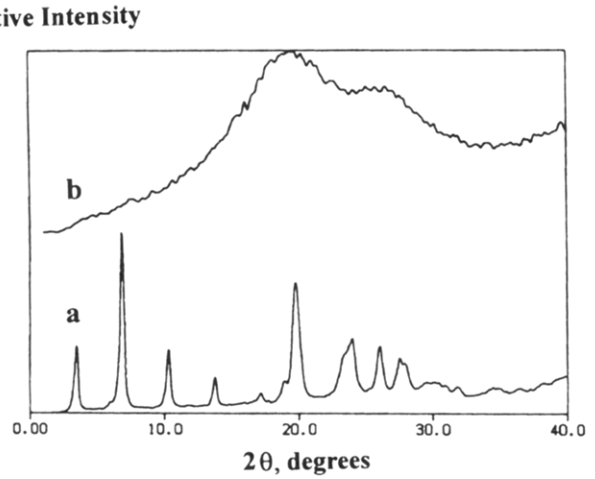

Figure 8. WAXD spectra of a plate (1 mm thick) of **1** before polymerization (a) and after heating for 1 h at 290 °C (b).

Table 5. Processing Conditions for 1–5

monomer	pressure (Psi)	temp (°C)	time (h)
1	1000	300	1.3
2	600–700	290	1.5
3	500	285	1.2
4	700–800	300	1.5
5	600–700	300	1.3

Scanning electron microscopy (SEM) was used in order to gain insight into the morphology of the polymer plates. SEM microphotographs of fracture surfaces of **3p** are shown in Figure 9. **3p** is void free and cohesive. The lack of proper processing parameters for **4** and **5** produced polymers with many voids; this is illustrated for **5p** in Figure 10. The existence of voids shows poor consolidation which significantly decreases the mechanical properties of these polymers. The ultimate properties of **4p** and **5p** can be determined only after the appropriate processing conditions are found.

Thermomechanical Properties. Dynamic mechanical analysis (DMA) was used for the evaluation of the thermomechanical properties of the processed polymers. The DMA data for **1p–5p** processed in the solid state are listed in Table 6. The temperature dependence of the flexural storage modulus, E', and tan δ for **2p** are shown in Figure 11. Table 6 shows that void-free **1p–3p** have almost the same E' (4.5–4.8 gPa) at room temperature. The rigid rod aromatic structures of the polyesters together with the high cross-link density are responsible for the very high E' values. These materials lose most of their crystallinity during polymerization, but they are still densely packed. Their moduli are much higher than those of amorphous cross-linked polymers. The higher E' values for **1p–3p** when compared to those for **4p** and **5p** are probably because **4p** and **5p** had some voids. **1p–3p** plates were dark brown with a reflective surface (voids <1 μm in diameter if any are present). These features indicate that satisfactory processing conditions (good combination of applied pressure, temperature, and processing time) have been developed. **4p** and **5p** plates were inhomogeneous. They had dark brown to light brown to light tan regions that coexisted in the polymer plates. The dark brown shiny surface indicates good consolidation. Even where the surface was light brown or tan it was found (using DSC and IR) that the matrix was completely polymerized. Thus the difference in the specimen color implies that the processing pressure was not ideal or that the pressure was not applied uniformly. The light colored, dull surface indicates scattering of the light due to voids in the plate (poor consolidation); these voids are responsible for the inferior thermomechanical properties of **4p** and **5p** (Table 6).

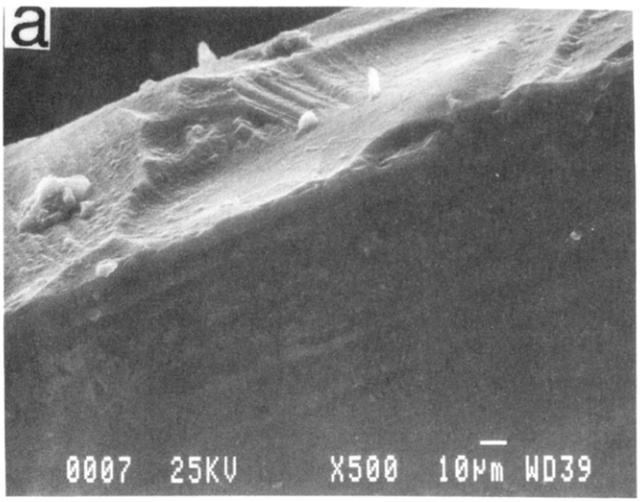

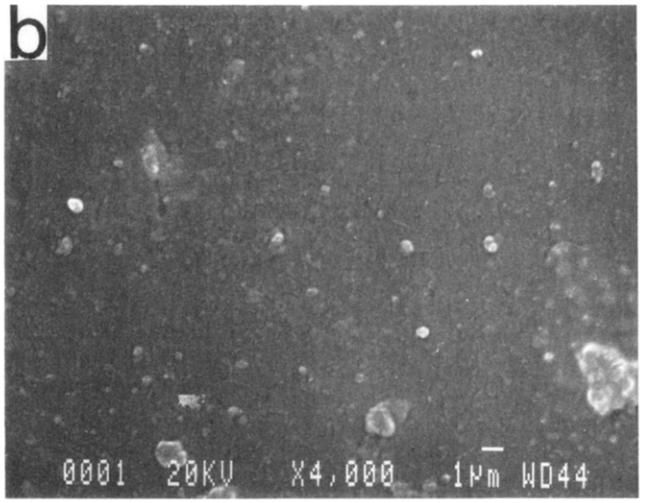

Figure 9. SEM microphotographs (fracture surface) for well consolidated **3p** (a) and (b).

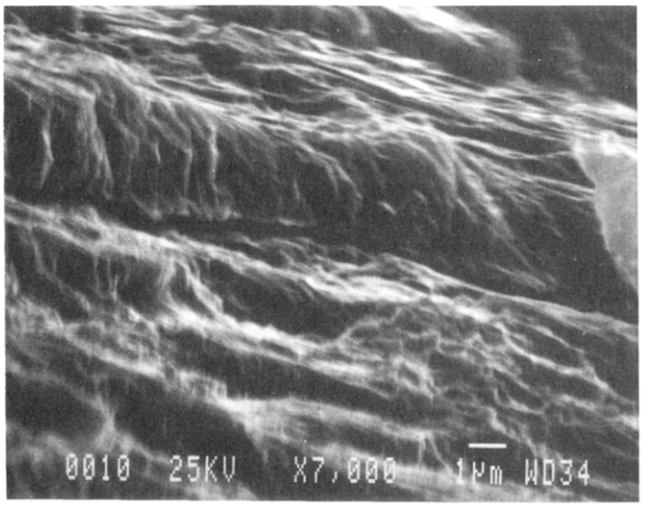

Figure 10. SEM microphotographs for poorly consolidated **5p** (fracture dull surface).

Table 6. Thermomechanical Data (DMA and TMA) for 1p–7p

polym	E′ (Gpa) room temp	E′ (Gpa) 200 °C	E′ (Gpa) 300 °C	T_g (°C)
1p	4.5	2.9	1.63	>415[a]
2p	4.5	3.0	1.70	344[a]
3p	4.8	2.9	0.8	290[a]
4p	3.8	3.1		349[b]
5p	3.1	2.6	2.3	>440[a]
6p				363[b]
7p				387[b]

[a] T_g determined by DMA (5 °C/min, 1-Hz frequency). [b] T_g determined by TMA (10 °C/min).

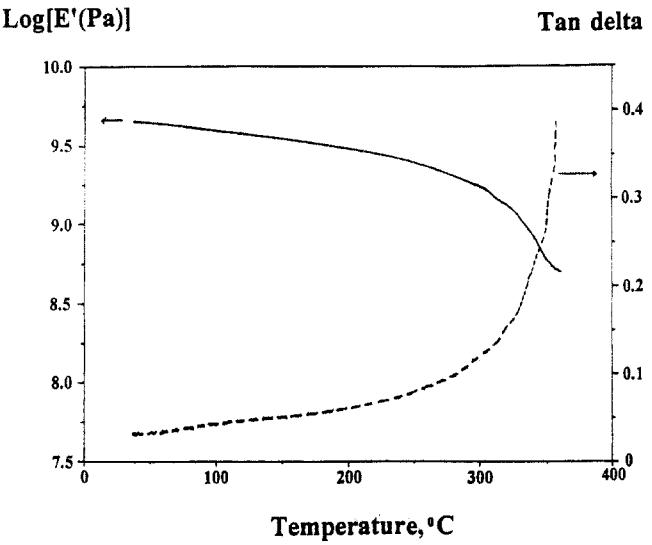

Figure 11. Temperature dependence of E' and tan δ for 2p.

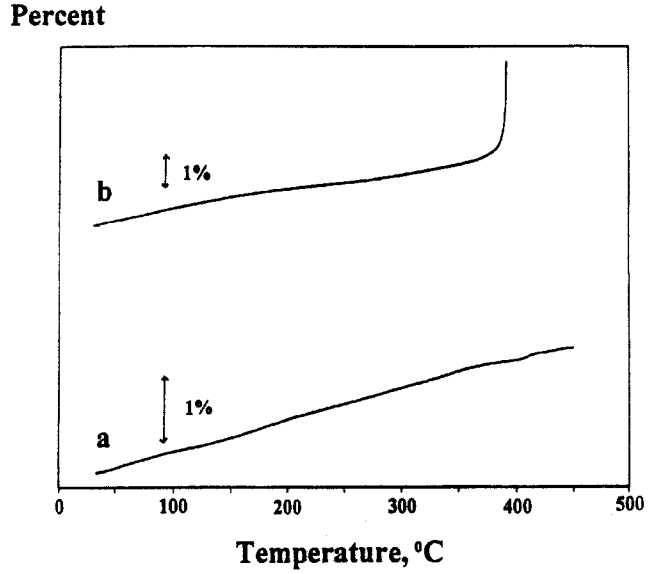

Figure 12. TMA thermograms for 6p (a) and for 7p (b).

DSC, TMA, and DMA techniques were used in order to define the T_g's of the polymers. However, using DSC the T_g's of the cross-linked resins could not be detected even after thermally cycling the same sample several times. Since 1p–7p are highly cross-linked, the change in C_p was very small.

Using thermomechanical analysis (expansion probe), TMA, the T_g's of 4p, 6p, and 7p were evaluated (the temperature where the polymer stops expanding linearly as it is heated from room temperature to 450 °C). The TMA thermograms for 6p and 7p are shown in Figure 12. Figure 12a shows that 6p expands 1.7% when it is heated from room temperature to 365 °C. The expansion is linear from 100 to 350 °C followed by a plateau from 350 to 425 °C. Its T_g was determined as 361 °C from the change in slope in the expansion curve. Figure 12b shows that 7p has a T_g of 387 °C and a linear thermal expansion of 2.5% when it is heated from room temperature to its T_g. Using DMA the T_g's of the polymers were determined as the maximum in tan δ as a function of temperature. From Table 6 it can be seen that all polymers (except 3p) had T_g's over 340 °C. 1p and 5p had T_g's over 415 °C. These polymers had T_g's 115 to 140 deg higher than their processing temperatures (Tables 5 and 6). 2p and 4p also had T_g's over 50 deg higher than their processing temperatures (Tables 5 and 6). These unusual results can be explained by considering that the acetylene groups of these monomers are packed into a very small fraction of the total volume. They interdigitate to a certain degree and polymerize well to high conversion without needing to diffuse to find other reactive ends. Thus high T_g's do not prevent high conversion at low temperatures. Linear liquid crystal monomers have been polymerized below their T_g's in the past. *p*-Acetoxybenzoic acid polymerized within minutes at 300 °C.[23] Crystalline needles of poly-*p*-benzamide were obtained by heating the monomer at 156 °C.[24] 5p had a T_g more than 90 deg higher than that of 4p (Table 6). Since 4p has four ester linkages instead of two, this significant difference in T_g is attributed to the higher cross-link density of 5p compared to that of 4p. By developing the appropriate processing conditions for 4p-7p it is expected that their T_g's will increase slightly while their storage moduli will increase very much. The polymers derived from polymerization of bis(4-(3-ethynylphenoxy)phenyl sulfone) or acetylene terminated phenylquinoxalines had T_g's[25] which varied from 300 to 365 °C, the highest reported in the literature for acetylene terminated polymers. Since 1p and 5p–7p had T_g's higher than those values, these polymers have the highest T_g values reported for acetylene terminated systems.

The tensile modulus for a poorly consolidated sample of 2p was measured and found to be 2.15 GPa at room temperature; its elongation at break was 0.67%. The stress–strain curve was a straight line up to break, as is expected for a highly cross-linked polymer: These values are much lower than the ultimate values because the specimens were not well consolidated and contained voids. It is well-known that the voids are stress concentrators and dramatically reduce the mechanical and thermomechanical properties of the polymers. The densities of well and poorly consolidated portions of the 2p specimens were measured in order to gain insight into the void percentage. Well consolidated (dark brown, shiny surface) 2p had a density of 1.26 g/cm^3. The density of tan, dull 2p was found to be 1.15 g/cm^3. Thus, some sections of the polymer had a 9% void volume.

Thermal Properties. Dynamic thermogravimetric analysis (TGA) in N_2 and air was used for the evaluation of the short term thermal and thermooxidative stability of 1p–7p. 1–7 were thermally polymerized as powders for 4 h at 260 °C in N_2. For comparative purposes 1–7 were thermally polymerized as powders for 2 h at 260 °C in air. The TGA data for 1p–7p polymerized in N_2 and air are listed in Tables 7 and 8. $T_{5\text{-}N/(\text{-}A)}$ indicates the temperature where the polymer cured in N_2 (or air) shows 5% weight loss. $PDT_{N/(A)}$ indicates the temperature of maximum decomposition rate for the polymer cured in N_2 (or air). It can be seen that $T_{5\text{-}A}$'s (Table 8) are higher than the corresponding $T_{5\text{-}N}$'s by 25–30 deg (Table 7). However PDT_A's (Table 8) are similar to or lower than those in N_2, PDT_N (Table 7). The anaerobic char yield at 800 °C, for

Table 7. TGA Data for 1p–7p Derived by Thermal Polymerization of 1–7 for 4 h at 260 °C in N_2

	nitrogen			air	
polym	$T_{5\%-N}$[a] (°C)	PDT_{-N}[b] (°C)	Y[c] (%)	$T_{5\%-N}$ (°C)	PDT_{-N} (°C)
1p	473	597	53	450	583
2p	416	562	41	422	572
3p	435	583	55	442	602
4p	415	579	43	410	588
5p	461	587	56	419	558
6p	420	562	54	441	582
7p	433	578	56	421	576

[a] Temperature where the polymer cured in N_2 shows a 5% weight loss. [b] Maximum decomposition temperature for the polymer cured in N_2. [c] Char yield at 800 °C.

Table 8. TGA Data for 1p–7p Derived by Thermal Polymerization of 1–7 for 2 h at 260 °C in Air

	nitrogen			air	
polym	$T_{5\%-A}$[a] (°C)	PDT_{-A}[b] (°C)	Y[c] (%)	$T_{5\%-A}$ (°C)	PDT_{-A} (°C)
1p	478	598	65	467	587
2p	460	558	63	429	560
3p	450	562	66	450	540
4p	458	576	60	454	546
5p	446	554	65	423	496
6p	485	562	65	447	563
7p	455	562	63	446	573

[a] Temperature where the polymer cured in air shows a 5% weight loss. [b] Maximum decomposition temperature for the polymer cured in the air. [c] Char yield at 800 °C.

the polymers cured in air, Y_A, is higher than the corresponding Y_N by 7–22% (Table 7). These results indicate that thermal polymerization in air yielded cross-linked resins with higher short term thermal stability than those polymerized in N_2. Comparing the anaerobic data (Table 8), one can seen that **6p** has the highest T_{5-A} and a very high char yield of 65% at 800 °C. **1p** has a slightly lower T_{5-A} (by 7 deg) and much higher PDT_A (over 35 deg) than those of **6p**. Both polymers have the same anaerobic char yield of 65% (800 °C). From these tests it can be concluded that **1p** is the most thermostable polymer. From Table 8 it can be seen that **1p** is also the most thermooxidatively stable polymer with the highest aerobic T_{5-A} and PDT_A of 467 and 587 °C. These results indicate that the biphenyl group has very high thermal and thermooxidative stability.

Since these polymers are to be used as films or polymeric plates in the atmosphere (air), the long term thermooxidative stability for **5p** (polymeric plate) was estimated using the isothermal aging technique (IGA). **5p** was chosen as a representative of this series of cross-linked esters. It was postcured for 2 h at 300 °C under N_2. **5p** lost about 30% of its initial weight after 100 h of isothermal aging at 320 °C in air. These IGA results indicate that these cross-linked polyesters can be used as load bearing materials only below 300 °C.

Experimental Section

Materials. Methylhydroquinone and chlorohydroquinone (Aldrich), were recrystallized from toluene. Hydroquinone (HQ) (Aldrich) was recrystallized in hot water in the presence of sodium sulfite. 4,4′-Dihydroxybiphenyl(AMOCO Corp.) was used as received. 1,5-Dihydroxynaphthalene (Lancanster Synthesis) was recrystallized from a water/methanol mixture in the presence of sodium sulfite. 2,6-Dihydroxynaphthalene and 4-(*N*,*N*-dimethylamino)pyridine, (Aldrich) were used as received. Terephthaloyl chloride (Aldrich) was recrystallized from hexanes. *p*-Ethynylbenzoyl chloride (EBC) was synthesized by a convenient, new, synthetic route developed in our laboratory.[18] Tetrahydrofuran (THF) (Fisher) was refluxed over sodium and distilled under nitrogen. Triethylamine (Fisher) was refluxed over KOH pellets and distilled under nitrogen.

Analytical Methods. Proton nulcear magnetic resonance (^1H NMR) spectra were taken on XL-200, 200-MHz FT-NMR. Chemical shifts (δ) are given in parts per million, with tetramethylsilane as the internal standard. Infrared spectra (FTIR) were recorded on a Bio-Rad Digilab FTS-60 spectrometer utilizing KBr pellets. Raman spectra were obtained on a DILOR XY Raman spectrometer with a CCD detector and laser power of 5.85 mW. Monomer and polymer densities were measured using a density gradient column containing potassium bromide in water. Pellets (20 mil thick) were made from the monomers by compression molding. For the corresponding polymers, films of similar thickness polymerized in the solid state under moderate pressure were used. X-ray scans were recorded using a Phillips APD 3520 automatic diffractometer. Nickel filtered copper Kα radiation was used. Scans were run from 1 to 40° with a goniometer speed of 2°/min. Thermal transitions were observed and hot stage cross-polarized photographs were taken on a Carl Zeiss optical polarizing microscope equipped with a Mettler FP-82 hot stage and a Mettler FP 80 central processor. HPLC was performed using an ISCO-HPLC instrument equipped with a UV detector which measured the absorbance at 254 nm with methanol as the eluting solvent at a flow rate of 1.0 mL/min. GPC was performed using a Waters GPC I equipped with a differential refractomonitor and a Hewlett Packard UV detector, with one precolumn (Plgel, 5μ, 100Å) and two Plgel columns (5 μm, 10 and 500 Å) with THF as the eluant at 1.0 mL/min flow rate. DSC was performed on a DuPont 2000 thermal analyzer with a heating rate of 15 °C/min in nitrogen at a flow rate of 50 mL/min. The TMA experiments were recorded on a DuPont 943 TMA using a 2- and 5-g expansion probe at 10 °C/min in static air. The DMA measurements were recorded on a DuPont 983 DMA and analyzed on a TA 2000 thermal analyzer. A ramp of 5 °C/min in N_2 (50 mL/min), 1-Hz frequency, 0.8-mm length correction, 0.16-mm amplitude, and a 0.38 Poisson's ratio were used. The tested samples were approximately 27 mm long, 9.6 mm wide, and 1.45 mm thick. The DMA tests represent an average value based on three tests. TGA measurements were performed on a DuPont 2100 thermal analyzer at 15 °C/min and a 50 mL/min gas flow rate. Microphotographs were taken on a JEOL 840A scanning electron microscope (SEM). Instron testing of polymeric samples was carried out on an Instron 1125 at room temperature with dog bone specimens with 23–29-mm reduced length, 5.7-mm width, 1.7-mm thickness, and a 0.05 mm/min cross-head speed. The stress–strain tests were performed in duplicate. There was considerable scatter in the individual values because the polymeric specimens were not uniform. The optimized processing conditions require an automatic heating press and a stainless steel tool mold with very small clearance. For this reason and because the polymer specimens prepared were not optimized on the basis of the above requirements, the values reported are preliminary and do not reflect the ultimate thermomechanical properties.

Neat Resin Processing. A cylindrical stainless steel tool mold of 5.5-cm inside diameter equipped with a thermocouple was sprayed with a high temperature release agent (Frekote 44) and dried at room temperature for 1 h. The mold was charged with approximately 4.5 g of monomer (powder) and pressed for 3 min under 8–10 kpsi at 90–100 °C. The mold was then placed into a preheated (processing temperature, Table 5) manually operated press (F. Carver, Inc.) under very low pressure (50 psi). The mold was heated at 20 °C/min heating rate. When the temperature of the mold reached 220–240 °C, the pressure listed in Table 5 was applied. After 1 h of heating and pressing, the pressure was released and the mold was cooled within 1–1.3 h. When the mold was at 60 °C or room temperature the plate was removed. In order to make plates of **6** and **7** which melt before polymerizing, a slightly different procedure was used. **6** was processed using the same mold. **6** (powder) was pressed in the mold under 8 kpsi for 4 min at room temperature. The pressure was released before heating to minimize extrusion of polymer through the die annulus. The mold was then heated for 1 h at 290 °C under 50 psi of pressure.

Isothermal Aging. Isothermal weight loss studies were conducted on the **5p** polymer plate (postcured for 2 h at 300 °C in N_2, five specimens with 0.2-, 0.2-, and 1.5-mm dimensions) at 320 °C ion an oven under 1 atm (static air).

1. Synthesis of 1–3 and 5–7. To a vigorously stirred solution of *p*-ethynylbenzoyl chloride (25.50 g, 155 mmol), in THF (400 mL) were added the aromatic diol (75 mmol) and 4-(*N*,*N*-dimethylamino)pyridine (0.93 g, 7.5 mmol) at room temperature. Upon dissolving the flask was placed in a water–ice bath (temperature range between 3 and 5 °C) and triethylamine (17.20 g, 170 mmol) was added gradually within 5 min. The reaction was exothermic. The mixture was stirred in the bath for 20 min and then stirred at room temperature for a further 8 h. Upon completion of the reaction, acetic acid (1.2 g, 20 mmol) was added to neutralize the excess triethylamine. Two-thirds of the solvent was then rotoevaporated, and the reaction mixture was poured onto crushed ice. It was filtered and stirred with 500 mL of water, then with 600 mL of a saturated solution of sodium bicarbonate, and again with water. After filtering, it was dried at 50 °C under vacuum. The monomers were obtained in high yield (93–99%) (see Table 1). Their purity was checked by GPC and ranged between 98 and 99.5% (Table 1). Their ^{1}H NMR data are given in Table 2.

2. Synthesis of 4. In a 500-mL three-necked flask equipped with a nitrogen inlet and calcium chloride drying tube, placed in an ice bath, were placed hydroquinone (14.54 g, 125.5 mmol) and THF (100 mL) and stirred. A solution of *p*-ethynylbenzoyl chloride (6.88 g, 42 mmol) in THF (60 mL) containing pyridine (4.3 g, 54.3 mmol) was added to the above solution dropwise over 40 min. The resulting mixture was stirred in the ice bath for 1 h and then at room temperature for a further 8 h. The solvent was rotoevaporated to a volume of 30 mL, and the mixture was poured over crushed ice. It was filtered, and the residue was stirred with 200 mL of water (twice) and then with 200 mL of warm water, filtered, and dried at 45 °C. The off-white crystalline material hydroquinone–mono(*p*-ethynylbenzoate) was obtained in 88% yield, mp 178–180 °C. The HPLC showed a single peak (purity 99%) with a retention time of 2.62 min. ^{1}H NMR (acetone-d_6): δ 3.32 (bs, 1H, –OH), 3.86 (s, 1H, ethynyl), 6.89 (d, 2H), aromatic ortho to –OH), 7.08 (d, 2H aromatic ortho to –OCO), 7.66 (d, 2H aromatic ortho to ethynyl), 8.14 (d, 2H aromatic ortho to –CO–).

To a vigorously stirred solution of hydroquinone-mono(*p*-ethynylbenzoate) (6.91 g, 29 mmol) in *N*,*N*-dimethylacetamide (70 mL) were added terephthaloyl chloride (2.94 g, 14.5 mmol) and 4-(*N*,*N*-dimethylamino)pyridine (0.18 g, 1.45 mmol). The clear solution was placed in a water–ice bath and triethylamine (4.11 g, 40.6 mmol) was added gradually within 2 min. The reaction was exothermic. After stirring for 10 min in the bath, the mixture was stirred at room temperature for 8 h and finally at 55 °C for 1 h. Acetic acid (0.8 g, 13.3 mmol) was added to neutralize the system. The solvent was rotoevaporated to a volume of 30 mL and poured over crushed ice. The mixture was centrifuged, and the residue was stirred with 150 mL of water (twice), filtered, and dried at 15 °C under vacuum. **4** (8.50 g) was obtained in 97% yield.

Summary and Conclusions

Seven new di-*p*-ethynylbenzoyl ester monomers (EBEs) were synthesized in high yield and high purity. Five of them polymerized in the solid state to yield highly cross-linked resins retaining gross order. Two polymerized in the nematic liquid crystal state. The difference between this and previously reported work on ethynyl terminated monomers or oligomers is that these monomers are liquid crystalline or crystalline during polymerization and yield polymers which retain their overall orientation and low order crystallinity. Because they polymerize in the solid state, they exhibit little or not polymerization shrinkage (0–2.3%). The modulus drops only slightly at the T_g because of the high cross-linking. EBEs polymerize to high conversion in spite of their rigid matrix because their lamellar organization brings all the ethynyl groups into a small volume. There may be further acceleration of the polymerization because of the interdigitation of their acetylene groups. The polymers had T_g's much higher than the polymerization temperature because EBEs are properly organized to polymerize in the solid state.

A new processing technique which invoves the solid state polymerization of rodlike cross-linked dioxyaryl–bis(*p*-ethynyl benzoates) under moderate pressure and heating has been developed. This technique was applied to monomers which neither melt nor have a softening point to yield cohesive, high modulus, high T_g polymers.

Because these polymer plates have high T_g's, high moduli, low thermal expansion, and very low polymerization shrinkage, they may be good candidates for high temperature composite matrices. Such composites should have good mechanical properties because the total matrix shrinkage for both polymerization and cooling from the reaction temperature is very low, thus minimizing the stress on the interfacial matrix–fiber bond.

Acknowledgment. Financial support by EPIC is gratefully acknowledged. The authors would like to thank Dr. Yaxim Wang from the Chemical Engineering Department (CWRU) for recording the Raman spectra and Mr. Daniel P. Scheiman (NASA Lewis Research Center, Laboratory 49) for recording the TMA thermograms.

References and Notes

(1) Litt, M. H.; Whang, W.; Yen, K.; Qian, X. *J. Polym. Sci., Polym. Chem. Ed.* **1993**, *31*, 183.
(2) Havens, S. J.; Hergenrother, P. M. *J. Polym. Sci., Polym. Chem. Ed.* **1984**, *22*, 3011.
(3) Takeichi, T.; Stille, J. K. *Macromolecules* **1986**, *19*, 2093.
(4) Takeichi, T.; Stille, J. K. *Macromolecules* **1986**, *19*, 2108.
(5) DeWinter, W.; Stein, R.; Urvents, H.; Masquelier, C. *J. Polym. Sci.* **1970**, *A1*, 8, 1955.
(6) Wolfe, J.; Loo, B.; Arnold, F. *Macromolecules* **1981**, *14*, 915.
(7) Stille, J. K. *Macromolecules* **1981**, *14*, 870.
(8) Gleiter, R.; Schaefer, W.; Eckert-Maksic, E. *Chem. Ber.* **1981**, *114*, 2309.
(9) Neeman, T.; Whitesides, G. *J. Org. Chem.* **1988**, *53*, 2489.
(10) Admur, S.; Cheng, A.; Wong, C.; Ehrlich, P.; Allendoerfer, D. *J. Polym. Sci., Polym. Chem. Ed.* **1978**, *16*, 407.
(11) Rato, J.; Dynes, P.; Hamermesh, C. *J. Polym. Sci., Polym. Chem. Ed.* **1980**, *18*, 1035.
(12) Hergenrother, P. M. *J. Macromol. Chem.* **1980**, *C19*, 1.
(13) Samyn, C.; Marvel, C. *J. Polym. Sci., Polym. Chem. Ed.* **1975**, *13*, 1095.
(14) Lucotte, G.; Cormier, L.; Delford, B. *J. Polym. Sci., Polym. Chem. Ed.* **1991**, *29*, 897.
(15) Hergenrother, P. M. *Macromolecules* **1981**, *14*, 891.
(16) Hergenrother, P. M. *Macromolecules* **1978**, *11*, 332.
(17) Wei, Y.; Hariharan, R.; Ray, J. *J. Polym. Sci., Polym. Chem. Ed.* **1991**, *29*, 749.
(18) Melissaris, A. P.; Litt, M. H. *J. Org. Chem.* **1992**, *57*, 6998.
(19) Barkalov, I.; Berlin, A.; Goldanskii, V.; Gao, M. *Vysokomol. Soedin.* **1963**, *5*, 368; *Polym. Sci. USSR (Engl. Transl.)* **1963**, *5*, 1025.
(20) Sandreczki, T.; Lee, C. *Polym. Prepr. (Am. Chem. Soc., Div. Polym. Chem.)* **1982**, *23*, (2), 185.
(21) Oleinic, E. F. In *Advances in Polymer Science*; Dusek, K., Ed.; Springer-Verlag: Berlin, **1986**; p 50.
(22) Kloosterboer, J. G. To be published (cited in: Hikmet, R. A.; Zwerver, B. H.; Broer, D. *J. Polymer* **1992**, *89*, 33).
(23) Economy, J.; Volksen, G. In *The strength and stiffness of polymers*; Zachariades, A. E., Porter, R. S., Eds.; Marcel Dekker: New York, 1983,; p 310.
(24) Morgan, P. W. *Macromolecules*, **1977**, *10*, 1381.
(25) Hergenrother, P. M. *Encyclopedia of Polymer Science and Engineering*; John Wiley & Sons: New York, 1985; Vol. 1, p 61.